Proceedings of the 2022 Design of Medical Devices Conference
DMD2022
April 11-14, 2022, Minneapolis, MN, USA

DMD2022-1025

DESIGNING A MURINE MODEL OF HUMAN GLIOBLASTOMA BRAIN TUMOR: DEVELOPMENT OF A PLATFORM FOR VALIDATION USING ULTRASOUND ELASTOGRAPHY

Griffin Mess
Johns Hopkins University
Baltimore, MD

Rasika Thombre
Johns Hopkins University
Baltimore, MD

Max Kerensky
Johns Hopkins University
Baltimore, MD

Eli Curry, PhD
Johns Hopkins University
Baltimore, MD

Fariba Abhabaglou, PhD
Johns Hopkins University
Baltimore, MD

Safwan Alomari
Johns Hopkins University
Baltimore, MD

Henry Brem, MD
Johns Hopkins University
Baltimore, MD

Nicholas Theodore, MD
Johns Hopkins University
Baltimore, MD

Betty Tyler
Johns Hopkins University
Baltimore, MD

Amir Manbachi, PhD
Johns Hopkins University
Baltimore, MD

ABSTRACT

Glioblastoma Multiforme (GBM) is a malignant brain cancer with low overall survival. Therefore, researchers are looking to augment its current therapeutic regimen, which includes surgical tumor resection, chemotherapy and radiation. A promising treatment modality, focused ultrasound, has been used as a non-invasive treatment for GBM through multiple approaches such as thermal ablation, immunomodulation, and blood brain barrier disruption. In order to develop these treatments for clinical trials, testing in animal models needs to be performed to investigate the efficacy of the treatment in complex biological environments, as well as to evaluate any side-effects. The more biologically relevant the animal model is to human anatomy, the more applicable the results will be for translation to clinical trials. Here, we report a human GBM rat model, which utilizes an IDH-wildtype, EGFRvIII mutant patient-derived xenograft in athymic rats. The in vivo tumor growth rate was assessed over a period of 20 days to evaluate reproducibility and to develop the model for future testing of FUS in the treatment of GBM.

Keywords: Glioblastoma, Neuro-oncology, Non-invasive, animal model, focused ultrasound

NOMENCLATURE

GBM	Glioblastoma Multiforme
FUS	Focused Ultrasound
HIFU	High Intensity Focused Ultrasound
PDX	Patient Derived Xenograft
UE	Ultrasound Elastography
SWE	Shear Wave Elastography
G	Shear Modulus
K	Bulk Modulus
ν	Poisson Ratio
Z	Acoustic Impedance
IDH	isocitrate dehydrogenase ½
DMEM	Dulbecco's Modified Eagle Medium
FBS	Fetal Bovine Serum
PBS	Phosphate Buffered Saline
EDTA	Ethylenediaminetetraacetic acid
MRI	Magnetic Resonance Imaging

1. INTRODUCTION

The most common form of primary malignant brain tumor is GBM [1]. The current standard of care includes a surgical tumor resection, typically followed by a combination of both chemo- and radiotherapy [2]. Minimizing damage to healthy central neural tissue while removing the entire tumor is exceptionally difficult, especially in deeper brain tumors, and typically results in GBM cells being left behind that can lead to recurrent cancer. In addition, resistance to both chemotherapy and radiotherapy is possible, and the adverse side effects of those treatments make quality of life difficult [4,5]. There are multiple preclinical treatments that are currently being explored.

Currently, there is a heavy focus on developing non-invasive therapies to treat brain cancers. Due to the emergence of new technologies that are being developed to treat GBM, it is imperative to develop reproducible and reliable in vivo experiments prior to implementation in clinical trials. Given the time and cost associated with bringing a medical technology to clinical trials, there exists a need to develop an animal model for testing GBM therapies. Animal models are important as they bridge the gap between the test tube and humans, providing a complex biological environment to show the efficacy of a treatment strategy as well as any potential side effects from the therapy. Due to their cost and availability, rodents are the ideal

animal model for emulating GBMs in humans. Accordingly, the development of human GBM tumors in rodents would provide a robust animal necessary to obtain approval for FDA clinical trials to test medical devices aimed at treating or eliminating GBMs. Previous in vivo studies testing medical devices for treating GBM have used rodent derived cells instead of human derived cells, leading to differences which makes results less robust [12].

One technology quickly becoming a leading approach for non-invasive surgery is focused ultrasound (FUS). Ultrasound transducers contain tiny piezoelectric crystals that vibrate when an electric field is applied, generating sound waves at incredibly high frequencies beyond the hearing range of humans. [6] The high frequency sound waves contain a lot of energy, and when the array of crystals is curved, the ultrasound waves converge into a small focal region that contains intense acoustic pressure and temperature. High Intensity Focused Ultrasound (HIFU), one of the many applications of FUS, is commonly used for thermal ablation. During HIFU treatment, high frequency ultrasound waves are focused onto a batch of tissue, causing that tissue's temperature to rise to become hyperthermal, which leads to coagulation necrosis [7].

Once the model is established, it would be pertinent for the purposes of FUS to establish various acoustic properties of the implanted tumor tissue. GBM tumors have differing mechanical properties than healthy brain tissue, which can have an effect on the FUS beam and its subsequent treatment results [13]. Once these properties are measured, it would be possible to simulate the intensity and temperature profiles of a sonication using mathematical models established in literature. The propagation of ultrasonic waves through tissue is governed by the tissue's elasticity, a measure of a medium's resistance to deformation. One way to measure a tissue's elasticity is via ultrasound elastography (UE). Shear wave elastography (SWE) is a technique where an ultrasound probe sends a longitudinal pulse wave through a tissue, inducing perpendicular shear waves across the tissue [14]. Recording the speed at which these shear waves travel enables one to approximate the elasticity of the tissue of interest. The shear modulus (G) of a tissue measures the resistance to deformation of a medium from the application of a shear wave, and can be characterized by the velocity of the shear wave c_s through a medium of a specific density ρ.

$$G = \rho {c_s}^2 \tag{1}$$

Ultrasound waves are longitudinal, and their elastic properties are governed by the inward force of a compression. The resistance to compression is quantified by the bulk modulus (K), which along with density governs the velocity (c) of an acoustic ultrasound wave traveling through a medium and can be derived using G from (1).

$$K = \rho c^2 - \frac{4G}{3} \tag{2}$$

Furthermore, there is a direct relationship between G and K, allowing for the conversion of shear to acoustic wave properties without needing to know the acoustic wave speed. This relationship is

$$K = \frac{2G(1+v)}{3(1-2v)} \tag{3}$$

where v is the Poisson ratio, a measurement of the deformation of a material in a direction perpendicular to the applied force. Soft tissues like brain matter and tumors, which are mostly made up of water, are thought of nearly incompressible and are thought to have Poisson ratios nearly $v \sim .5$ [14]. Because of this, K in the brain is magnitudes higher than G. Acoustic impedance (Z), a measure of the resistance that a tissue has to the propagation of ultrasound through it, can then be derived using the results from (2) or (3) using the relationship

$$Z = \sqrt{K\rho} \tag{4}$$

Acoustic impedance is an important measurement for prediction of ultrasound reflection, which can occur at the boundaries of two tissues with impedance mismatches. The fraction of reflected acoustic intensity at the boundary of two tissues with differing impedances Z_1 and Z_2 is

$$R = \left(\frac{Z_2 - Z_1}{Z_2 + Z_1}\right)^2 \tag{5}$$

UE has already been used in clinical studies for assistance in finding the brain-tumor boundaries and residual tissue. This was shown to be more accurate than without the use of UE [13]. UE has even been used during HIFU experiments to monitor the development of induced lesions [14]. This shows that UE has relevancy in FUS beyond the elastic properties of tissue. SWE is integrated into many different clinical ultrasound systems such as the Canon Aplio i800 and Philips EPIQ, so it has high ease of access. Additionally, collecting UE data is relatively simple and quick as it involves taking a B-Mode image and then drawing a ROI around the tissue of interest before executing a built-in UE paradigm. UE applied to an *in vivo* animal tumor model has the potential to help optimize future FUS treatments.

In this experiment, we present a novel rat model using orthotopic GBM patient-derived xenografts (PDX) and a method to track the progression of these tumors over time. Additionally, UE techniques were applied to *ex vivo* intact whole mouse brains with implanted tumor from the same PDX cell line. The acoustic properties mentioned were measured or derived for proof of concept. The development and characterization of this human GBM murine model provides a beneficial experimental platform for future neuroengineers to accelerate the testing of new medical devices.

2. MATERIALS AND METHODS

Ethics Statement

All experimental procedures were approved by the Johns Hopkins Medical Institute Animal Care and Use Committee

(Protocol Number: RA20M97), and conducted in accordance with the National Institutes of Health guidelines for the care and use of laboratory animals.

2.1 Glioblastoma Cell Line Cultivation

All liquid reagents and disposables were purchased from Thermo Fisher Scientific (Waltham, MA) unless otherwise stated. The PDX GBM cell line Mayo59 (M59) was commercially purchased from the Mayo Clinic in Rochester, MN. The cell line was originally collected from an 83-year-old female woman with a primary IDH-wildtype glioblastoma tumor in the right temporal lobe. This cell line arose from a gain of function mutation of the epidermal growth factor receptor variant III (EGFRvIII) gene. A gain of function deletion in axons 2-7 of the EGFR gene causes overexpression of EGFRvIII, which is common in GBM tumors and has shown increased proliferation, angiogenesis, invasiveness, and reduced apoptosis through a variety of pathways [16]. These qualities make this cell line ideal for the establishment of a GBM animal model. The cells were cultured in DMEM, fortified with 10% FBS and 1% Penicillin/Streptomycin, and then cultured in a humidified incubator at 37°C with 10% CO_2.

Cells were grown out in T-75 flasks and cells that had a passage number of < 10 were used for this experiment. On the day of implantation, cells were washed with PBS and then 0.25% trypsin/EDTA was added to each flask to suspend the cells. In order to determine if the number of cells were sufficient, a small sample of cell media solution was added to a hemocytometer (Hausser Scientific, Horsham, PA) for cell counting. Once the number of cells was quantified, they were spun down using a Sorvall Legend X1R centrifuge (Thermo Fisher) at 500 RPM for 5 minutes, the supernatant was removed, and the cells were transferred to a 1.5 ml microcentrifuge tube (Eppendorf, Hamburg, Germany) on ice.

2.2 Tumor Cell Implantation

Fisher 344 female athymic rats, 125-175 grams, rats (Charles River Laboratories, Wilmington, MA) were used for this experiment. Each rat was anesthetized using 75 mg/kg ketamine (Henry Schein, Melville, NY), and then the area surrounding the surgical site was treated with betadine solution (Henry Schein, Melville, NY). An incision was made in the head along the sagittal suture line from the middle of the ears down to just before the eyes. Fascia was scraped away around the incision until the sagittal suture line, the lambda, and bregma were visualized. A micromotor high speed rotary drill (Foredom Electric Co, Bethel, MA) was used to create a small burr hole big enough for a 10 uL Hamilton Syringe (Hamilton Company, Reno, NV) to fit in between the lambda and bregma and to the left of the sagittal suture line. The rat was then placed on a stereotactic frame and 1.5 x 10^6 cells were injected at a depth of 3.5 mm into the brain. The rat was then removed from the frame and the incision closed using a wound stapler. Rats were monitored until they awoke from anesthesia.

2.3 Monitoring of Rat Behavior and Tumor Growth

Rats injected with M59 cells were monitored to assess behavior and neurological function. Each rat was weighed, and rat health and behavior were observed at regular intervals, with any abnormal behavior denoted. On the 10th and 20th day following implantation, each rat underwent T2 MRI scans in a 9.2 Tesla MRI machine to monitor tumor growth. MRI scans were made in the coronal and sagittal planes for each rat. The MRI scans from each rat, on each day of imaging, were uploaded into ImageJ, where the metadata from the scans was used to measure approximate tumor volume. For each slice, the tumor boundaries were identified and traced in the imaging software. To determine tumor volume, a 3D ROI-based interpolation method was used [17]. The area of each tumor trace was identified, and then the total area was summed over each slice. Finally, the total area was multiplied by the distance between slices (1 mm).

2.4 *Ex Vivo* Elastography

A NOD/SCID female mouse (Charles River Laboratories) was implanted with M59 cells in a similar method described above. The mouse was monitored for tumor growth. Once the tumor reached significant size, the mouse was euthanized, and the brain containing the M59 tumor resected and placed in a 10% buffered formalin phosphate solution (Fisher Scientific, Hampton, NH). After a week, the tumor was removed from the formalin solution for elastography. A Canon (Ota City, Tokyo, Japan) Aplio i800 ultrasound machine was used to capture images. The i18LX5 probe (5-18 Hz) was initiated in the 'SPINE' preset for shear wave elastography (SWE). The brain was surrounded by Medline (Northfield, IL) Blue Ultrasound Gel for acoustic coupling to the transducer. The shear wave propagation and acoustic velocity profiles of the ultrasound waves were captured. A sagittal planar orientation was chosen to exhibit as much of both normal brain tissue and tumor tissue possible. For each image, B-mode ultrasound images were taken to locate the brain and tumor tissue. A ROI box was drawn around the whole brain including the tumor, and then the stiffness and velocity of a shear wave was recorded in the ROI.

2.5 Calculation of Acoustic Properties

An example sample is illustrated for a proof-of-concept demonstration for collection of acoustic properties (Figure 5). For each image taken, a potential sampling methodology of a circular region was chosen from known sections of both the healthy mouse tissue and the M59 tumor. The acoustic velocities of a single equivalent region in both the brain tumor and healthy tissue were independently averaged. Using a literature value for the density of solid GBM brain tumor tissue and a density equivalent to water for healthy tissue, elastic moduli, the acoustic impedance, and the acoustic reflection of both tissues were derived. These values were calculated based on equations 1-5.

3. RESULTS AND DISCUSSION

The goal of these experiments was to develop a human tumor model in rodents that has high lethality, high reproducibility and could be used to test non-invasive glioblastoma treatments *in vivo*. Here, we show that after injecting the M59 glioblastoma cells into the rats, tumors began to form. Figure 1 shows the growth and development of these tumors in all three rats after 10- and 20-days post implantation.

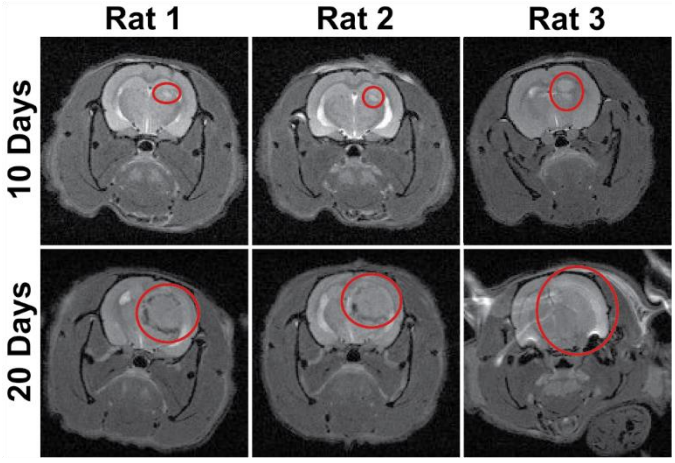

FIGURE 1: REPRESENTATIVE CORONAL VIEW T2 MRI IMAGES OF THREE RATS IMPLANTED WITH PDX GLIOBLASTOMA CELLS (MAYO 59), 10- AND 20-DAYS POST-IMPLANTATION. RED ELLIPSOIDS INDICATE WHERE TUMORS ARE GROWING.

After 10 days, rats 1 and 2 show small, asymmetrically placed circular masses that are different in consistency than the surrounding tissue. Additionally, both tumors are located approximately 3.5 mm into the tissue within the line of the skull puncture site. After 20 days, the tumor masses are much larger and more obvious on MRI. The calculated tumor volumes can be seen in Figure 2.

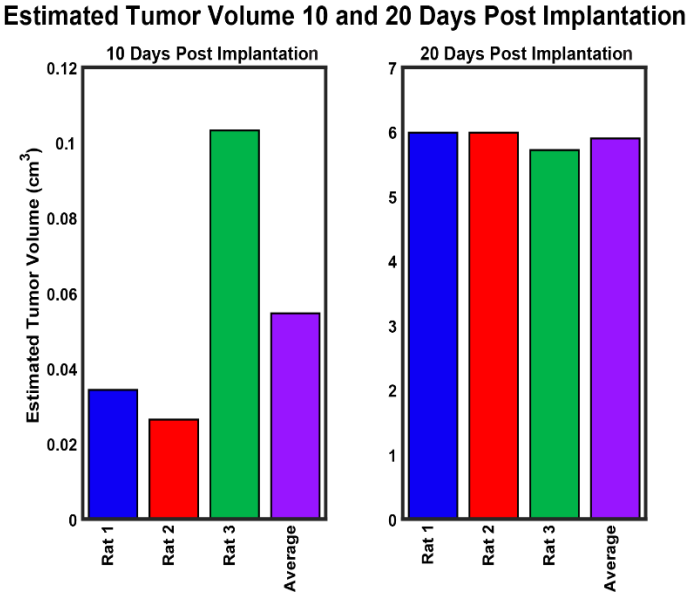

FIGURE 2: ESTIMATED TUMOR VOLUME OF EACH RAT BASED ON THE MRI SCANS TAKEN AT DAYS 10 AND 20 POST IMPLANTATION. TUMOR VOLUMES WERE ESTIMATED USING A 3D INTERPOLATION METHOD. THE AVERAGE OF THE THREE TUMOR VOLUMES IS ALSO DISPLAYED.

Each rat had large tumors with subsequent midline shifts. For rat 3, the cells appeared to have been implanted in closer proximity to the left ventricle of the brain than in the other two rats. This allowed the tumor to grow and expand into the ventricle, causing it to grow more rapidly. As can be seen in the Day 10 data for Figure 2A, the tumor in rat 3 has a significantly larger volume than in rats 1 and 2. Additionally it is important to note that the location of the tumor in rat 3 caused hydrocephalus. By Day 20, the tumor in rat 3 occupied the entirety of the left hemisphere of the brain. Interestingly, by Day 20, the other two tumors caught up to the tumor in rat 3 in terms of volume. This most likely is due to the exponential growth of this tumor *in vivo* demonstrating its viability and lethality. The tumors in rats 1 and 2 were eventually able to arrive at the ventricles and proliferate into open space, achieving the same size as the tumor in rat 3 as well as leading to hydrocephalus. This result demonstrates the continuity in the how this tumor line grows when implanted in a rat model. However, it is important to note that Rat 3 had significant neurological disorders and had to be euthanized by day 22, which was much earlier than the other two rats.

Additionally, the weights of each animal were tracked to see if they were consistent with the development of a tumor. It was hypothesized that the animals would gain weight until the tumors became a significant size, and then the rats would lose weight as they succumbed to the disease brought on by the tumor. The weights of each rat were tracked, starting from the date of implantation to end of life. Figure 3 shows the progression of the weights of the animals.

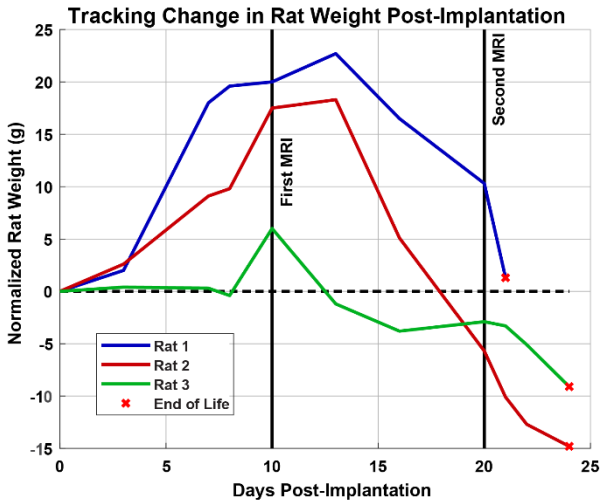

FIGURE 3: TRACKING THE CHANGE IN WEIGHT OF EACH RAT POST IMPLANTATION. WEIGHTS ARE NORMALIZED BY SUBRACTION OF THEIR WEIGHTS ON DAY OF IMPLANTATION. IT IS DENOTED WHEN THE MRI OCCURRED AS SHOWN IN FIGURE 1, AS WELL AS THE END POINT FOR EACH RAT.

The weights of the rats followed the predicted trend of an initial increase followed by a sharp decrease, consistent with tumor growth. By the date of the first MRI, each rat was around its peak weight, and then tumors grew to a size significant enough to cause weight loss. By the second MRI, each of the rats were at much smaller weights than their peak weights.

UE results had significant variability from capture to capture and one of the snapshots is seen in the figure 4. The authors do not claim that this capture is representative of all other images taken; rather, Figure 4 serves as a demonstration of the methodology of obtaining acoustic properties using SWE on the mouse brain and human GBM tumor.

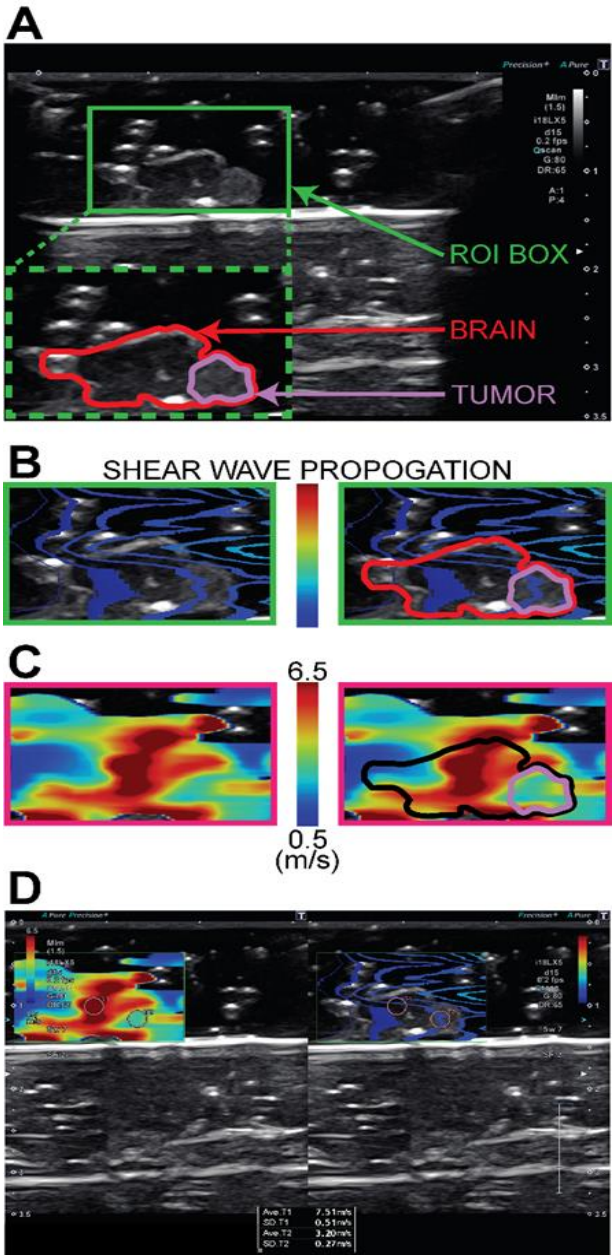

FIGURE 5: STAGES OF IMPLEMENTING AND EVALUATING ULTRASOUND SHEAR WAVE ELASTOGRAPHY. (A) 'B-MODE' ULTRASOUND IMAGE WITH AN APPROXIMATE OUTLINE OF THE FULL BRAIN (RED), TUMOUR (PURPLE), ROI OF FUTURE ELASTOGRAPHY (GREEN). (B) PROPOGATION OF THE SHEAR WAVE (C) SPEED HEAT MAP OF SHEAR WAVES PROPOGATION THROUGH THE TISSUE IN FOCUS. (D) POST-PROCESSING AND DATA CAPTURING METHODS FOR AVERAGE SHEAR WAVE SPEED AND STANDARD DEVIATION.

Although it is unlikely that the healthy neural tissue of the rat would exhibit different stiffness as compared to the mouse brain tissue, we have definitively shown here that the tumors can grow in both types of immunocompromised rodents. The mouse brain and implanted tumor used to make Figure 4 can be seen in figure 5. The tumor tissue appeared as a pinker tissue, and appeared lighter on B-mode ultrasound images than normal tissue, making it relatively easy to find.

FIGURE 4: TOP VIEW OF THE *EX VIVO* RESECTED MOUSE BRAIN CONTAINING M59 IMPLANTED TUMOR, WITH SIZE COMPARISON. TUMOR TISSUE IS HUED PINK ON THE RIGHT FLANK OF THE BRAIN.

As this is an ex vivo experiment of an organ that has been stored in a preservative, no conclusions of definitive acoustic values can be made at this time. However, in this specific case, the shear wave speed at the artificially selected regions, as well as calculated acoustic properties from equations 1-4, in both the M59 tumor model and healthy tissue can be seen in table 1. A v=.45 was chosen from literature.

Tissue	M59 Tumor	Brain Tissue
Density (kg/m^3)	1035[18]	1000
Averaged Shear Wave Velocity (m/s)	3.20 (.27)	7.51 (.51)
Shear Modulus (KPa) (1)	10.60	56.40
Bulk Modulus (KPa) (3)	102.45	545.20
Acoustic Impedance (kPa*s/m^3) (4)	10.30	23.35
Percentage of Acoustic Reflection at tumor boundary (5)	15.04%	

TABLE 1: MEASURED AND DERIVED SHEAR AND ACOUSTIC PROPERTIES OF INTRACRANIALLY GROWN M59 GBM TUMOR AND HEALTHY MOUSE BRAIN TISSUE. M59 TUMOR DENSITY WAS FOUND IN LITERATURE [18], AND BRAIN TISSUE DENSITY WAS ASSUMED EQUIVALENT TO WATER. NUMBERS IN PARENTHESES REFER TO EQUATION WHERE IT WAS DERIVED FROM. NUMBERS IN PARENTHESIS INDICATE STANDARD DEVIATIONS.

In this instance, the difference in speed of the propagating shear waves might indicate an expected stiffness differential between the healthy and cancerous tissues, although these values do not represent the elasticity profiles that living tissue would exhibit. Tumors are characteristically stiffer than healthy tissue, so these values are against our initial hypothesis. Additionally, the bulk modulus is known in soft tissues to be 4 to 5 magnitudes higher than the shear modulus [19]. Using the speed of sound in water, 1540 m/s, the bulk moduli result in 2.45 x 10^9 KPa and 2.37 x 10^9 KPa in the tumor tissue and healthy tissue respectively. This would suggest a ν that is extremely close to .5 if the values for G are valid. As this is only a singular case of tissue that has been fixed and without the presence of blood and other biological fixtures, the values obtained here are not for reference and only to show the feasibility of using this method for planning experiments with various ultrasound therapies. Future *in vivo* experiments using this cell line and animal model would be able to accurately measure these values.

The feasibility of creating a human GBM rodent model for *in vivo* research has been demonstrated through these preliminary data. The efficiency of creating this tumor model is key, as implanting tumors is a time-consuming and expensive process. In this study, the M59 GBM tumor grew well in all three rats. Although one of the tumors grew faster than the others, all three tumors ended up reaching the same endpoint. The M59 tumor cells were incredibly invasive and proliferative, making them ideal for repeatability. The month-long overall survival and predictable behaviors of the rat's post-implantation allow for a standardized model with behavioral, weight, and tumor size checkpoints. Those checkpoints could be used as benchmarks for *in vivo* therapy experiments to determine if the therapies are successfully treating tumors.

4. CONCLUSION

As GBM research expands, it is important to have *in vivo* experiments that are as close to a clinical setting as possible. Promising non-invasive treatments for GBM, such as FUS, require extensive research before they can be brought to clinical trials. Here, we reported on a rodent model using a PDX GBM cell line, which can be used to standardize the study of non-invasive GBM treatments prior to implementation in a clinical trial. We also attempted to determine the elastic properties of the tumor, which is important for planning future ultrasound experiments. With this new rat model, researchers can accelerate the testing of novel medical devices such that they can be brought to clinical trials in a or expeditious manner.

ACKNOWLEDGEMENTS

The authors acknowledge funding support from the National Science Foundation (NSF) STTR Phase 1 Award (#: 1938939), 6 © 2021 by ASME Defense Advanced Research Projects Agency (DARPA) Award (#: N660012024075), and Johns Hopkins Institute for Clinical and Translational Research (ICTR)'s Clinical Research Scholars Program (KL2), administered by the National Institutes of Health (NIH) National Center for Advancing Translational Sciences (NCATS).

In addition, Dr Henry Brem is a paid consultant to Insightec and chairman of the company's Medical Advisory Board. Insightec is developing focused ultrasound treatments for brain tumors. This arrangement has been reviewed and approved by the Johns Hopkins University in accordance with its conflict-of-interest policies.

• Research Funding from NIH, Johns Hopkins University, and philanthropy

• Consultant for CraniUS, Candel Therepeutics, Inc., InSightec*, Accelerating Combination Therapies*, Catalio Nexus Fund II, LLC*, LikeMinds, Inc*, Galen Robotics, Inc.* and Nurami Medical* (*includes equity or options)

REFERENCES

[2] Batash, R., Asna, N., Schaffer, P., 2017, "Glioblastoma Multiforme, Diagnosis and Treatment; Recent Literature Review," Current Medicinal Chemistry, 24(27) pp. 3002-3009.

[3] Tan, A. C., Ashley, D. M., López, G. Y., 2020, "Management of Glioblastoma: State of the Art and Future Directions," CA: A Cancer Journal for Clinicians, 70(4) pp. 299-312.

[4] Oliver, L., Lalier, L., Salaud, C., 2020, "Drug Resistance in Glioblastoma: Are Persisters the Key to Therapy?" Cancer Drug Resistance, 3.

[5] De Bacco, F., D'Ambrosio, A., Casanova, E., 2016, "MET Inhibition Overcomes Radiation Resistance of Glioblastoma Stem-like Cells," EMBO Molecular Medicine, 8(5) pp. 550-568.

[6] Fishman, P., and Frenkel, V., 2017, "Focused Ultrasound: An Emerging Therapeutic Modality for Neurologic Disease," Neurotherapeutics, 14(2) pp. 393-404.

[7] Belzberg, M., Mahapatra, S., Perdomo-Pantoja, A., 2020, "Minimally Invasive Therapeutic Ultrasound: Ultrasound-Guided Ultrasound Ablation in Neuro-Oncology," Ultrasonics, 108pp. 106210.

[9] Huszthy, P. C., Sakariassen, P. Ø, Espedal, H., 2015, "Engraftment of Human Glioblastoma Cells in Immunocompetent Rats through Acquired Immunosuppression," PLoS ONE, 10(10) .

[10] Chan, H. W., Uff, C., Chakraborty, A., 2021, "Clinical Application of Shear Wave Elastography for Assisting Brain Tumor Resection," Frontiers in Oncology, **11**pp. 619286.

[11] Sigrist, R. M. S., Liau, J., Kaffas, A. E., 2017, "Ultrasound Elastography: Review of Techniques and Clinical Applications," Theranostics, 7(5) pp. 1303-1329.

[12] Geoghegan, R., Ter Haar, G., Nightingale, K., 2021, "Methods of Monitoring Thermal Ablation of Soft Tissue Tumors - A Comprehensive Review," Medical Physics (Lancaster), .

[13] An, Z., Aksoy, O., Zheng, T., 2018, "Epidermal Growth Factor Receptor and EGFRvIII in Glioblastoma: Signaling Pathways and Targeted Therapies," Oncogene, 37(12) pp. 1561-1575.

[14] Kim, H. J., and Kim, W., 2012, "Method of Tumor Volume Evaluation using Magnetic Resonance Imaging for Outcome Prediction in Cervical Cancer Treated with Concurrent Chemotherapy and Radiotherapy," Radiation Oncology Journal, 30(2) pp. 70-77.

[15] Dahiya, S., Chaudhury, K., and Singh, V. R., 1997, "Ultrasonic studies on malignant and benign brain tumors, in vitro," Anonymous IEEE, 2, pp. 832-834 vol.2.

[16] Emelianov, S. Y., Aglyamov, S. R., Karpiouk, A. B., Oct 2006, "1E-5 Synergy and Applications of Combined Ultrasound, Elasticity, and Photoacoustic Imaging (Invited)," Anonymous IEEE, pp. 405-415.